February 10, 2000

MEMORANDUM TO: Jack R. Strosnider, Director
Division of Engineering

FROM: William H. Bateman, Chief ***/ra/***
Materials and Chemical Engineering Branch

SUBJECT: AUTHORIZATION TO PRESENT AND PUBLISH TECHNICAL PAPERS

Simon C. F. Sheng and Matthew A. Mitchell have authored a paper titled, "PTS Screening Criteria Revisited and Its Implication to the Master Curve Approach." In addition, Simon C. F. Sheng has authored a second paper titled, "The Applicability of Thin-wall Limit-Load Solutions to Stainless Steel Piping Used in the Nuclear Industry." Both were accepted for presentation at the 2000 International Conference on Nuclear Engineering (ICONE-8). Simon Sheng and Matthew Mitchell will attend the meeting on April 2-6, 2000, and Simon Sheng will make the presentations. This memorandum is to request your concurrence for presentation and publication of the subject papers presuant to NRC Management Directive 3.9.

We believe that the NRC staff participation in the subject meeting will be extremely useful in promoting the exchange of information among the participants concerning the PTS evaluations and the use of limit-load analysis in piping flaw evaluations.

Attached is a copy of the subject papers. The conference program has not been published yet. Expenses are expected to be about $200 for each author, not including the registration fee.

Approval: ***/ra/*** ***2/11/00***
Jack Strosnider, Director
Division of Engineering

Attachments: As stated

CONTACT: Simon Sheng, EMCB/DE
415-2708

MEMORANDUM TO: Jack R. Strosnider, Director
Division of Engineering

FROM: William H. Bateman, Chief
Materials and Chemical Engineering Branch

SUBJECT: AUTHORIZATION TO PRESENT AND PUBLISH TECHNICAL PAPERS

Simon C. F. Sheng and Matthew A. Mitchell have authored a paper titled, "PTS Screening Criteria Revisited and Its Implication to the Master Curve Approach." In addition, Simon C. F. Sheng has authored a second paper titled, "The Applicability of Thin-wall Limit-Load Solutions to Stainless Steel Piping Used in the Nuclear Industry." Both were accepted for presentation at the 2000 International Conference on Nuclear Engineering (ICONE-8). Simon Sheng and Matthew Mitchell will attend the meeting on April 2-6, 2000, and Simon Sheng will make the presentations. This memorandum is to request your concurrence for presentation and publication of the subject papers presuant to NRC Management Directive 3.9.

We believe that the NRC staff participation in the subject meeting will be extremely useful in promoting the exchange of information among the participants concerning the PTS evaluations and the use of limit-load analysis in piping flaw evaluations.

Attached is a copy of the subject papers. The conference program has not been published yet. Expenses are expected to be about $200 for each author, not including the registration fee.

Approval: _____
Jack Strosnider, Director
Division of Engineering

Attachments: As stated

CONTACT: Simon Sheng, EMCB/DE
415-2708

DISTRIBUTION:
EMCB RF File Center

DOCUMENT NAME: G:\EMCB\SHENG\ICONE8.WPD

INDICATE IN BOX: "C"=COPY W/O ATTACHMENT/ENCLOSURE, "E"=COPY W/ATT/ENCL, "N"=NO COPY

OFFICE	EMCB:DE	E	EMCB:DE	E	EMCB:DE	E	D:DE	N
NAME	SSheng:CFS		MMitchell:MAM		KWichman:KRW		WBateman:WHB	
DATE	2 / 9 /00		2 / 10 /00		2 / 10 /00		2 / 10 /00	

OFFICIAL RECORD COPY

ATTACHMENT

Proceedings of ICONE 8
8th International Conference on Nuclear Engineering
April 2-6, 2000, Baltimore, MD USA

ICONE-8691

PTS SCREENING CRITERIA REVISITED AND ITS IMPLICATION TO THE MASTER CURVE APPROACH

Simon C.F. Sheng **Matthew A. Mitchell**

U.S. Nuclear Regulatory Commission
Material and Chemical Engineering Branch
7D4, OWFN, USNRC, Washington D.C. 20555
Phone: (301) 415-2708
Fax: (301) 415-2444
E-mail: SHENG@NRC.GOV

ABSTRACT

The information regarding the determination of the pressurized thermal shock (PTS) screening criterion of 270°F for axial welds, the 2-sigma margin of 60°F, and the limiting vessel failure frequency of $5X10^{-6}$ is about 17 years old. The 1982 PTS study, documented in SECY-82-465, discussed all of these parameters. However, this document does not contain detailed information regarding the derivation of these frequently cited values. As a result, the perception about their origins and physical meanings may not be consistent among engineers and scientists who are interested in the methodology of estimating embrittlement of reactor pressure vessel materials. This paper revisits the determination of these three values from the 1982 PTS study. The objective is two-fold: first, to present the origins of these frequently cited numbers from a historical point of view, and second, to connect the deterministically determined PTS screening criterion for axial welds and the generically derived margin of 60°F to the probabilistic fracture mechanics (PFM) results from the 1982 PTS study. Further, the authors will examine the shift margin, σ_{Δ}, from a probabilistic point of view using the PFM results from a recent plant-specific analysis. This paper also makes a comparative study of the current methodology and the master curve approach and presents two hypotheses regarding the relationship between these two approaches.

INTRODUCTION

The United States Nuclear Regulatory Commission (USNRC) began to actively address the issue of pressurized thermal shock (PTS) for United States reactors in the late 1970s and early 1980s. The PTS event, of which thermal loads caused by the rapid cooling of the fluid in contact with the reactor pressure vessel (RPV) inside wall are postulated to couple with pressure and preexisting flaws, may potentially challenge RPV integrity. The Rancho Seco event that occurred in 1978, as documented in SECY-82-465 (1982), demonstrated that significant PTS events could occur and accelerated the development of the necessary analysis tools. By 1981-1982, the USNRC staff and the reactor vendors performed sufficiently detailed evaluations of several actual events and probabilistic studies regarding hypothetical event sequences to serve as the basis for the screening criteria established in the USNRC's "PTS Rule," Title 10 of the Code of Federal Regulations Part 50 Section 61 (10 CFR 50.61) published in 1986. Additional work has been completed since the early 1980s to address certain aspects of the PTS study and some modifications have been made to 10 CFR 50.61 in 1992 and 1997. A full-scale reevaluation by the USNRC is currently underway, but not yet completed. Hence, the original early 1980s work documented in SECY-82-465 stands as the principal basis for the PTS Rule today.

THE PTS RULE

The analysis of SECY-82-465 represents the most comprehensive generic evaluation of PTS for U.S. facilities that has been carried out to date by the USNRC. This evaluation concluded that appropriate screening criteria could be based on the projection of the inside diameter (ID) nil-

ductility reference temperature (RT_{NDT}) for each RPV material. The analyses supported the selection of 132.2 C (270.0 °F) as the screening value for axial (longitudinal) welds and base materials and 148.9 C (300.0 °F) for circumferential (girth) welds. These screening values would later be incorporated into 10 CFR 50.61 issued in 1986 (the 1986 Edition of 10 CFR 50.61), in which a material's RT_{NDT} at the end of license (EOL) would be termed RT_{PTS}. The general methodology for determining material RT_{NDT} values was developed by the Ad Hoc Working Group on the Selection of RT_{NDT} Values and was calculated as the sum of the initial RT_{NDT}, the shift of RT_{NDT} (ΔRT_{NDT}) due to irradiation, and a margin (M) to account for uncertainties in initial RT_{NDT} values, copper and nickel contents, fluence, and the calculational procedures. The ΔRT_{NDT} is referred in the PTS Rule as ΔRT_{PTS}. The derivation of the screening criterion of 270°F for axial welds, the associated 2-sigma margin of 60°F, and the limiting vessel failure frequency of $5X10^{-6}$ is addressed in the following.

The Generic Initial RT_{NDT} and Its Associated Margin σ_I

The initial RT_{NDT} was determined in accordance with the testing methodology given in the American Society for Mechanical Engineers (ASME) Code, Section III, Paragraph NB-2331 of the summer 1972 addenda. This methodology relies on Charpy V-notch and Drop Weight tests to establish the initial RT_{NDT} of a material. For vessels fabricated prior to the testing requirements of the summer 1972 addenda, the USNRC has recognized alternative methodologies in USNRC Branch Technical Position MTEB 5-2. These alternative methodologies address initial RT_{NDT} determination when insufficient Charpy V-notch and Drop Weight test data exist. Finally, generic Initial RT_{NDT} values for some classes of materials have been established and, in some cases, these generic values have been included in 10 CFR 50.61.

The Ad Hoc Working Group recognized that in many cases licensee vessels had been fabricated prior to the 1972 Edition of the ASME Code and that insufficient Charpy and/or Drop Weight data existed from the actual vessel materials to make a determination of the initial RT_{NDT}. It was proposed that the limited data that was available for plate and forging materials was to be used in conjunction with MTEB 5-2 to arrive at a conservative initial RT_{NDT} for these materials. For the RPV weld materials, however, the Working Group acquired 82 weld test data from Combustion Engineering (CE) and 10 from Babcock and Wilcox (B&W) and proposed that generic values be used for two "classes" of welds: -49°C (-56°F) for weld manufactured using Linde 0091, 1092, 124, or ARCOS B-5 fluxes (CE), and -18°C (0°F) for welds manufactured with Linde 80 flux. These values were included in the 1986 Edition of 10 CFR 50.61 and continue to be used today.

In examining the weld material Initial RT_{NDT} database, the Working Group observed that the standard deviation σ_I for the larger data set from the Linde 0091, 1092, 124, and ARCOS B-5 flux welds was 9.4°C (17°F) and this value was assumed to also represent the σ_I for Linde 80 flux welds. Therefore, a value of 9.4°C (17°F) was assigned for σ_I if a generic initial RT_{NDT} value was used. The 1986 Edition of 10 CFR 50.61 introduced the use of 0°C (0°F) if a material-specific initial RT_{NDT} value was available, however, the use of 0°C (0°F) for σ_I was not discussed in either the recommendations of the Working Group nor in the SECY report.

Between 1986 and the present, other classes of material have been identified and other generic initial RT_{NDT} values have also been developed based on considerations similar to those outlined above. For these more recently defined generic classes of material, other σ_I values have been developed and applied in a limited number of cases. It was recognized that the use of a generic value introduces additional uncertainty and the margin term in the PTS evaluation is increased to account for this additional uncertainty when generic initial RT_{NDT} values are used.

The Trend Curve for ΔRT_{NDT} and Its Associated Margin σ_Δ

For PTS evaluation, SECY-82-465 recommended use of the lower RT_{PTS} value stemming from two methodologies for assessing the impact of radiation damage on RPV materials. The first methodology was based on the work done for the USNRC by George Guthrie (1982). The second was based on the upper bound curve of Regulatory Guide 1.99, Revision 1 (1977).

Guthrie proposed a mean trend curve based on approximately 177 PWR surveillance data:

$$\Delta RT_{PTS} = (-10 + 470\ Cu + 350\ Cu\ Ni) * (f / 10^{19})^{0.27} \qquad (1)$$

where Cu is the weight percent copper, Ni is the weight percent nickel, and f is the fluence (E > 1 MeV) in neutrons / cm^2.

The standard deviation, σ_Δ, of the surveillance data using the above mean trend curve is 13.3°C (24°F). It will be shown later that this σ_Δ had been used to derive the final margin of 33.3°C (60°F) for the PTS study of axial welds discussed in SECY-82-465.

For materials with high copper and nickel contents, the Guthrie mean trend curve was found to be conservative with respect to the Upper Limit Curve published in Regulatory Guide (RG) 1.99, Revision 1, given by the form:

$$\Delta RT_{PTS} = 283\ (f / 10^{19})^{0.194} \qquad (2)$$

Since this curve was found to bound the available data, its use in lieu of the Guthrie curve was justified for some materials. The final determination of the applicable embrittlement model as proposed in SECY-82-465 was to be the lesser RT_{PTS} value from these two trend curves and their respective margins. It should be noted that the σ_Δ is zero for the RG methodology because the trend equation is for the upper bound curve.

However, the trend curve used in the probabilistic analyses, from which the limiting vessel failure frequency of $5x10^{-6}$ was derived, was neither of the two methodologies. The one used was the early version of the Guthrie equation:

$$\Delta RT_{PTS} = (-4.83 + 476\ Cu + 267\ Cu\ Ni) * (f / 10^{19})^{0.218} \quad (3)$$

Although SECY-82-465 did not mention the σ_Δ value associated with this early version of the Guthrie mean trend curve, the authors believe it should be close to 24°F, judging from the close similarity of Eqs. (1) and (3).

The original PTS rule was published in 1986. Since then, additional work in the area of radiation damage assessment has been performed. In May 1988, the USNRC published Revision 2 to RG 1.99, which incorporated separate models for predicting the radiation embrittlement of base materials and weld metals using the same PWR surveillance database that Guthrie used. These revised models were subsequently incorporated into 10 CFR 50.61 in its 1992 Edition and remain current today. The ΔRT_{PTS} is calculated from:

$$\Delta RT_{PTS} = CF * FF \quad (4)$$

where the chemistry factor CF is determined from separate tables for weld and base metals provided in 10 CFR 50.61. The fluence factor FF is calculated from:

$$FF = f^{(0.28 - 0.10*\log(f))} \quad (5)$$

and f is the fluence (E > 1.0 MeV) at the RPV clad-to-base metal interface.

The 1992 Edition of 10 CFR 50.61 also permitted the use of meaningful plant-specific surveillance data results (via the guidance in Regulatory Guide 1.99, Revision 2) for calculating ΔRT_{PTS} (the CF part) in lieu of using the general correlations.

It should be pointed out that the models of Guthrie and RG 1.99, Revision 2 were based on a relatively small set of surveillance data points (approximately 177) when compared to the number which have been acquired from U.S. surveillance program through early 1997 (approximately 600 to 700). Therefore, ongoing work to reevaluate this expanded database is being pursued by the USNRC staff and may result in improved models of radiation embrittlement for future revisions of 10 CFR 50.61.

The Margin M

The concept of an additional term to be added to account for uncertainties in establishing RT_{PTS} or RT_{NDT} originated from the Ad Hoc Working Group on the Selection of RT_{NDT} Values. The methodology proposed by the Working Group and incorporated into SECY-82-465 recognized two contributions to this uncertainty term: (1) σ_I, the standard deviation from the analysis of initial RT_{NDT} determinations made on RPV-type weld materials; and, (2) σ_Δ, the standard deviation of the embrittlement database from the Guthrie mean curve. Mathematically, it took the following form:

$$M = 2\sqrt{(\sigma_I^2 + \sigma_\Delta^2)} \quad (6)$$

Applying Eq. (6) to welds having the generic initial RT_{NDT} of -49°C (-56°F) with the σ_I of 9.4°C (17°F) and using the Guthrie mean trend curve of Eq. (1) with the σ_Δ of 13.3°C (24°F), results in a final margin M of 32.8°C (59°F). This was the basis of SECY-82-465 for using the margin of 33.3°C (60°F) in estimating the limiting vessel failure frequency.

When the separate embrittlement models for weld and base metals were introduced in Revision 2 of RG 1.99, the standard deviation σ_Δ of the weld embrittlement data around the weld model was determined to be 15.6°C (28°F) and the σ_Δ of the base metal data around the base metal model was determined to be 9.4°C (17°F). However, per Rg 1.99, Revision 2, these values could be reduced by 50 percent if credible plant-specific surveillance data was used as the basis for the material's CF instead of that from the tables of the RG. For completeness, the commonly used margin values, according to RG 1.99, Revision 2, are summarized in Table 1.

Table 1. Most Commonly Used Margins According to RG 1.99, Revision 2

	Initial RT_{NDT}	σ_I (°F)	Shift	σ_Δ (°F)	Margin (°F)
Plate	Generic	17	Table	17	48
			Credible Surv.	8.5	38
	Measured	0	Table	17	34
			Credible Surv.	8.5	17
Weld	Generic	17	Table	28	66
			Credible Surv.	14	44
	Measured	0	Table	28	56
			Credible Surv.	14	28

The Selection of 270°F as the PTS Screening Criterion

SECY-82-465 identified eight actual overcooling transients as potential PTS initiators. Based on about 350 total PWR reactor years operating experience in the United States, the USNRC made a plot (Fig. 2-14 of the SECY) of the cumulative frequency per reactor year of events as a function of the final fluid temperature of the transient (T_f). In the meantime, the USNRC had performed deterministic fracture mechanics calculations for each of the eight events to determine critical RT_{NDT} values for crack initiation. A similar frequency plot (Fig. 4-1 of the SECY) was developed to represent the cumulative frequency per reactor year of events as a function of the critical RT_{NDT} values. For a nominal event frequency of

10^{-2} per reactor-year, these two figures gave values of approximately 260°F and 280°F, respectively. A compromise between the two values was 270°F. The event frequency of 10^{-2} per reactor-year was not a result from a rigorous analysis. In the words of SECY-82-465: The justification for choosing 10^{-2} is only that this is comfortably lower than the range of "anticipated operating occurrences."

Since the 270°F screening criterion was chosen, the two figures mentioned above have been corrected for earlier errors in the interpretation of the experienced events. The event frequency has been revised from10^{-2} per reactor-year to 9x 10^{-3}.

The results from Probabilistic Fracture Mechanics Analyses

In SECY-82-465, the USNRC also developed what was at that time a ground-breaking study using the probabilistic risk assessment (PRA) for evaluating vessel integrity issues. This action was significant in that it permitted the USNRC to examine the impact of postulated low frequency event sequences on vessel integrity and to examine the changes in specific parameters of the beltline material such as crack size, copper content, fluence value, fracture toughness, and initial RT_{NDT} value to the results of probabilistic fracture mechanics (PFM) calculations.

The tool used by USNRC in generating PFM results summarized in SECY-82-465 was the VISA code (1983). VISA is a computer code based on PFM methodology that performs millions of deterministic vessel simulations, or Monte Carlo simulations, to determine the conditional probability of failure (POF) for a vessel subjected to a specific transient. A failed vessel was defined as a vessel having a crack that grew to the maximum depth of 70 percent of the wall thickness, or reached the state of plastic instability. The vessel conditional POF is the ratio of the number of failed vessels to the number of simulations. For each simulation, the specific parameters mentioned above were treated as random variables and were assigned values according to the prescribed distributions specified by the user. The vessel failure frequency, the ultimate parameter of interest, is simply the result of the conditional POF times the event frequency of the input transient.

To select the critical transients for bounding analyses, the USNRC worked with the Westinghouse Owners Group (WOG) to identify all appropriate probabilistic risk assessment event sequences which could lead to a PTS event. With some consultation with the WOG, the USNRC finally narrowed the list of transients to four events which could lead directly to a PTS challenge: steamline breaks, steam generator tube ruptures, small loss-of-coolant accidents (LOCA), and extended high-pressure injection (HPI). The PFM results were summarized in a single figure (Figure 8-3 of the SECY or Figure 1 of RG 1.154), where the vessel failure frequency was plotted as a function of mean surface RT_{NDT} for each of the four transients. A curve designated as "PRA TOTAL" was also shown in the figure, which was the numerical sum of the vessel failure probabilities for all four transients. This figure is reproduced here in Fig. 1.

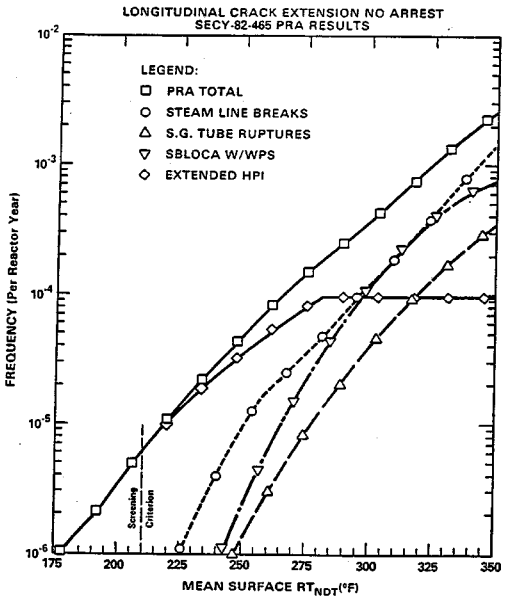

Figure 1 SECY-82-465 PRA Results

The authors would like to point out a key element in the methodology that is related to the master curve fracture toughness methodology to be discussed later. The RT_{NDT} value, which has been discussed frequently, was used for indexing the crack initiation fracture toughness (K_{Ic}) and crack arrest fracture toughness (K_{Ia}) curves, the early version of the ASME K_{Ic} and K_{Ia} curves, to obtain the appropriate K_{Ic} and K_{Ia} values for the fracture mechanics analysis in vessel simulations.

The Limiting Vessel Failure Frequency of $5X10^{-6}$

So far, we have introduced all three parameters needed for estimating the limiting vessel failure frequency for longitudinal welds: (1) the SECY-82-465 results plotted as the vessel failure frequency versus mean surface RT_{NDT} for four critical transients, (2) the screening criterion of 270°F determined from the deterministic fracture mechanics analysis, and (3) the margin of 60°F derived from the σ_I of 17°F based on 82 weld data from Combustion Engineering and Babcock & Wilcox and the σ_Δ of 24°F based on fitting approximately 177 PWR surveillance data to Guthrie's mean trend curve of Eq. (1). Subtracting the margin of 60°F from the screening criterion of 270°F, one obtains the limiting mean surface RT_{NDT} of 210°F. Figure 1 shows that the limiting vessel failure frequency (ordinate), corresponding to the mean surface RT_{NDT} of 210°F (abscissa) for the PRA curve labeled as "PRA TOTAL", is $5X10^{-6}$. This is the limiting vessel failure frequency that has been referenced in numerous publications.

A STUDY ON σ_Δ USING PLANT-SPECIFIC DATA

10 CFR 50.61 states, "M means the margin to be added to account for uncertainties in the values of $RT_{NDT(U)}$, copper and nickel contents, fluence and the calculational procedures." As discussed previously, this general margin M has two components, σ_I and σ_Δ. The σ_Δ was derived from PWR surveillance data fitted to Guthrie's mean trend curve. Its derivation has nothing to do with the study on probability of vessel failure documented in SECY-82-465. The statement from 10 CFR 50.61 reflected qualitatively that unirradiated and irradiated data that had been used in deriving σ_I and σ_Δ were from numerous test specimens.

In 1994, the USNRC studied the implication of applying σ_Δ of 28°F specified by RG 1.99, Revision 2 to RPV welds with high variabilities in copper and nickel as part of the review of the PTS issue for a nuclear power plant. Conventionally, σ_Δ was treated as a constant in the RPV pressure-temperature limits evaluation and the PTS evaluation using the screening criteria. This time, the USNRC approached the σ_Δ from an opposite direction and treated it as a variable. The USNRC used the reported mean values for copper, nickel, and fluence for the limiting beltline material of that plant and treated them as random variables in the VISA PFM simulations. The standard deviation of copper had been varied from 0.025%, the value used in SECY-82-465, to 0.075%, the standard deviation for this plant-specific weld. A median value of 0.050% had also been simulated. The standard deviation of nickel had been set to be either 0.0%, the value used in SECY-82-465, or 0.1275%, the standard deviation for this plant-specific weld. Further, the standard deviation of fluence had been set to be either 0% or 20% of the mean value. The above combinations gave seven cases.

The USNRC used VISA-II.D (1991) to perform the random selection of copper, nickel, and fluence values according to the input mean and standard deviation values for the assumed normal distribution. However, instead of going to the VISA-II.D routines for the PFM calculations, the USNRC revised the program to register the mean RT_{NDT} value for each simulation until one thousand simulations had been made for each case. A statistical analysis was then performed to determine the standard deviation of these one thousand mean RT_{NDT} values. The results are shown in Fig. 2. One may notice that the standard deviations for four cases exceed the current RG value of 28°F. This is not surprising because the variation of copper and nickel for this plant-specific case is exceptionally high. For instance, the copper variation used in this study is three times the value that was employed in SECY-82-465. In addition, SECY-82-465 did not consider the variation of nickel at all. Nonetheless, a higher σ_Δ should be used for the PTS evaluation for this plant. The staff eventually used VISA-II.D to perform a complete PFM analysis to predict vessel failure frequency for this plant and thus had considered the proper σ_Δ implicitly. This PFM analysis is documented in a safety evaluation by USNRC (1995).

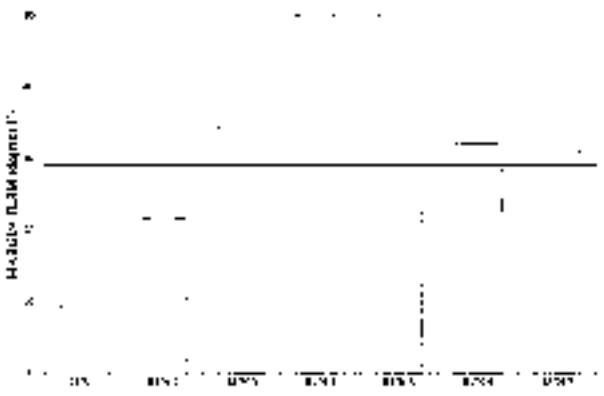

Figure 2 A Study on σ_Δ Using Plant-specific Data

IMPLICATION OF THE PTS RULE TO THE MASTER CURVE APPROACH

It was mentioned briefly that the RT_{NDT} value was used for indexing the crack initiation fracture toughness (K_{Ic}) and crack arrest fracture toughness (K_{Ia}) curves to obtain the appropriate K_{Ic} and K_{Ia} values for the fracture mechanics analysis in deterministic or probabilistic vessel integrity simulations. In recent years, a different approach, the master curve fracture toughness methodology, has been proposed. Instead of using the indexing parameter RT_{NDT}, which is based on the results from drop weight and Charpy V-notch tests as defined in the ASME Code, this new methodology proposed to use an alternative index, T_0, which is directly measured from fracture toughness tests according to ASTM E 1921 - 97 (97). With T_0, the master curve method can define a median fracture toughness curve, or a fracture toughness curve of any specified tolerance bound for the material under evaluation. The fracture toughness curves with 1, 2, 3, 4, 5, and 10% for the lower bound and 90, 95, 96, 97, 98, and 99% for the upper bound are readily available in E1921-97. The term "Master Curve" was originated from the fact that all ferritic steels have the same fracture toughness curve that differed only in their location on the temperature scale.

This paper examines the idea of replacing a portion and, possibly, the entirety of the current PTS methodology by the master curve method. The authors compare, in terms of depth and scope, the engineering work that has been done and might need to be done for the master curve method with the technical work behind the current PTS methodology. In principle, both methodologies relied on a test-based "material constant," i.e., RT_{NDT} for the current method and T_0 for the Master Curve method, to represent the varying fracture toughness for these materials at different temperatures. The master curve method was brought one step closer to the current approach philosophically when another parameter RT_{T0} was defined in ASME Code Case N-629 as

$$RT_{T0} = T_0 + 35°F \quad (7)$$

With this relationship, the 5% lower bound fracture toughness curve from the master curve method can be compared directly to the ASME K_{Ic} curve, of which the corresponding median ASME K_{Ic} curve was used in deterministic and probabilistic vessel integrity analyses supporting the current PTS rule.

Because of this similarity, an approach to replace only the necessary portion of the current PTS methodology by the master curve method so that the vast amount of work which has been done to the current PTS methodology needs not to be repeated makes great sense. Along this line, two hypotheses can be made. The prerequisite for the continued discussion of the hypotheses is that the fracture toughness, K_{Jc}, from specimens of various thickness up to above 8T is relevant to the K_{Ic} of the vessel wall about eight inches thick. For a discussion of this relevance, please see the work by Sokolov et al. (1997) and the work by Wallin (1999).

Hypothesis 1

The measured $\triangle RT_{NDT}$ value is a good representation of the change in the fracture toughness due to irradiation and can be related to $\triangle RT_{T0}$. Consequently, the master curve method using the current trend curve can be applied.

Basis and Comments

The determination of $\triangle RT_{NDT}$ is different from the determination of the initial RT_{NDT}. The $\triangle RT_{NDT}$ determination involves only Charpy tests as opposed to Drop-weight and Charpy tests for the initial RT_{NDT} determination and only one criterion ($\triangle RT_{NDT}$ at 30 ft-lb) as opposed to the dual criteria of 50 ft-lb and 35 mils lateral expansion for the initial RT_{NDT} determination. The one-test and one-criterion determination of $\triangle RT_{NDT}$ greatly reduced the probability of incurring errors in the process of testing and data processing and, therefore, the measured $\triangle RT_{NDT}$ may be a good representation of the embrittlement effect. Consequently, there might be a relationship between $\triangle T_0$ and $\triangle RT_{NDT}$. This hypothesis has been substantiated somewhat by the work of Sokolov and Nanstad (1996), whose work showed the following relationship:

$$\triangle T_0 = \triangle RT_{NDT}, \text{ for welds, and} \quad (8)$$

$$\triangle T_0 = 1.16 \triangle RT_{NDT}, \text{ for base metals.} \quad (9)$$

The corresponding σ_Δ is approximately 13°C (23.4°F) for welds and 18°C(32.4°F) for plates. It should be noted that since RT_{T0} differs from T_0 by a constant, $\triangle RT_{T0}$ is the same as $\triangle T_0$.

Table 2 makes a comparison of the key parameters of the current methodology with those of the master curve method. The lightly shaded areas under the heading "Master Curve" represent places where work similar to that underlying the current PTS rule has been performed. Specifically, Kirk (1999) established some generic T_0 values for certain classes of materials, and his applying the fluence function of RG 1.99, Rev. 2 to $\triangle RT_{T0}$ data was in line with Hypothesis 1 that the measured $\triangle RT_{NDT}$ value under the realm of the current PTS rule is a good representation of the change in the fracture toughness due to irradiation. Kirk's work was similar to that underlying the current PTS rule, however, σ_I and σ_Δ for the database of RT_{T0} and $\triangle RT_{T0}$ that were analyzed by him were only presented implicitly in his figures. It should be noted that the database (32 data points) used by Kirk for establishing generic T_0 and σ_I values for certain classes of materials, is much smaller that those (82 data points) used in the current PTS rule. Further, the database (~50 data points) used by Kirk for establishing (implicitly) σ_Δ value for a combined database of weld and plate materials, is also much smaller that those (177 data points) used in the current PTS rule. Hence, the issue of whether more data should be acquired, and how much more, for the acceptance of the master curve method under Hypothesis 1 as an alternative to the current PTS rule is likely to become a subject of debate.

When material-specific initial RT_{NDT} values are available, the current methodology allows the use of 0°F for σ_I. The basis is that the generally conservative nature of using RT_{NDT} to index the K_{IC} curve brings with it less emphasis on the exact determination of σ_I. While it may be proposed that the uncertainty associated with the determination of T_0 from ASTM E1921-97, σ_{T0}, provides an appropriate reference for the uncertainty to be used in a PTS evaluation using the master curve method, this may not be sufficient. What remains to be demonstrated, in the opinion of the authors, is what additional uncertainty, if any, must be added when extending the results of testing a small section of a surveillance weld or a small piece of plate material to characterize the properties of the corresponding material in an RPV. A metallurgical understanding of the variability (under relevant fabrication conditions and controls) in the microstructual species which contribute to the fracture behavior of these materials must be brought to bear in order to provide an adequate solution to this problem. The same issue is relevant to the case where an irradiated RT_{T0} is determined. However, it is more difficult for the irradiated case because additional uncertainty regarding the irradiation response of the surveillance material versus the irradiation response of the actual RPV material must also be accounted for.

The heavily shaded areas under the heading "Master Curve" represent places where work similar to those underlying the current PTS rule has not been started yet. It was mentioned above that the defining of RT_{T0} as T_0 plus 35°F in ASME Code Case N-629 made a direct comparison possible between the 5% lower bound fracture toughness curve of the master curve and the ASME K_{Ic} curve of the current PTS rule. Since the difference is not insignificant, it is meaningful to revise the screening criteria and the limiting vessel failure frequency using the 5% lower bound fracture toughness curve of the master curve.

Hypothesis 2

The master curve method should stand on its own without referencing any work underlying the current PTS rule.

Basis and Comments

Figure 3-4 of draft TR-108390, Rev.1 depicts that the T_0 values for a wide range of materials spread uniformly in a range from -150 to 30°F, while the RT_{NDT} values tend to form two clusters at about 0 and 50°F. This indicates that when the fracture toughness curve varies evenly in a certain range for these materials, the conventional RT_{NDT} approach can only measure two fracture toughness characteristics. This casts some doubt on the use of the Charpy test and the even less controllable drop-weight test to extract fracture toughness information from specimens, unirradiated or irradiated. Consequently, the master curve method might need to stand on its own without referencing any work underlying the current PTS rule.

In the discussion of the use of the master curve method under Hypothesis 1, the authors mentioned that there might be a need to establish a new screening criterion for T_0, and new PFM results plotted as vessel failure frequency versus mean surface T_0. Thus, the only additional work to be done for the use of the master curve method under Hypothesis 2 versus Hypothesis 1 is the development of a new trend curve using all data available for $\triangle T_0$. One byproduct of this effort is the determination of $\sigma_{\triangle}$, which, when combined with σ_I, can be used with the new screening criterion to determine the new limiting vessel failure frequency.

CONCLUSION

This paper revisited the three important parameters underlying the current PTS rule: the screening criterion of 270°F for axial welds, the 2-sigma margin of 60°F, and the limiting vessel failure frequency of $5X10^{-6}$. The review of the derivations of these parameters gives us implications about the work needed to be accomplished for any proposed alternative. One possibility is to revise the three parameters along the similar underlying philosophy of the current PTS rule using expanded database, a better fracture mechanics methodology, and a new trend curve based on a better fitting of the surveillance data. Using the master curve method is another possibility. The authors have presented two hypotheses regarding the application of the master curve method. One application intended to replace the current PTS rule partially and the other application intended to replace the current PTS rule completely. The authors have examined the engineering work underlying the current PTS rule and the work that has been accomplished so far for the master curve method. For each hypothesis, new areas which might need some attention and areas which might need additional work for the application of the master curve method have been highlighted for discussion so that we are in a better position to assess the use of the master curve method as an alternative to the current PTS rule.

ACKNOWLEDGMENTS

The authors are grateful to Jack Strosnider, William Bateman, Keith Wichman, and Mark Kirk of USNRC for their valuable comments on this paper.

REFERENCES

American Society for Testing and Materials, 1997, "Standard Test Method for Determination of Reference Temperature, T_0, for Ferritic Steels in the Transition Range," E 1921 - 97, ASTM, West Conshohochen, Pennsylvania.

Electric Power Research Institute, 1998, "Application of Master Curve Fracture Toughness Methodology for Ferritic Steels," Draft report TR-108390, Revision 1, EPRI, Palo Alto, California.

Guthrie, G.L., and McElroy, W.N., 1982, "LWR Pressure Vessel Surveillance Dosimetry Improvement Program: Quarterly Progress Report January 1982 - March 1982," NUREG/CR-2805, Volumn 1, (HEDL-TME 82-18), Hanford Engineering Development Laboratory, Richland, Washington.

Kirk, Mark, and Lott, Randy, 1999, "Initial Reference Temperatures and Irradiation Trend Curves for Use with RT_{T0}, a Preliminary Assessment," PVP-Vol. 393, ASME, New York, New York.

Sokolov, M.A., Wallin, K., and McCabe, D.E., 1997, "Application of Small Specimens to Fracture Mechanics Characterization of Irradiated Pressure Vessel Steels," ASTM STP 1321, ASTM, West Conshohochen, Pennsylvania.

Sokolov, M.A. and Nanstad R.K., 1996, "Comparison of Irradiation-Induced Shifts of K_{Jc} and Charpy Impact Toughness for Reactor Pressure Vessel Steels," ASTM STP 1325, 18th International Symposium on Effects of Radiation on Materials, Hyannis, Massachusetts.

U.S. Nuclear Regulatory Commission, 1995, "Safety Evaluation by the Office of Nuclear Reactor Regulation Related to the Evaluation of the Pressurized Thermal Shock Screening Criteria for Palisades Plant," U.S. Nuclear Regulatory Commission, Washington, D.C.

U.S. Nuclear Regulatory Commission, Policy Issue from J.W. Dirks to NRC Commissioners, 1982, "Enclosure A: NRC Staff Evaluation of Pressurized Thermal Shock, November 1982," SECY-82-465, U.S. Nuclear Regulatory Commission, Washington, D.C.

U.S. Nuclear Regulatory Commission, 1977, "Effects of Residual Elements in Predicting Radiation Damage to Reactor Vessel Materials," Regulatory Guide 1.99, Revision 1, U.S. Nuclear Regulatory Commission, Washington, D.C.

VISA-II.D, 1991, Letter Report from Simonen, F.A. to Mayfield, M.E., Including Articles on Residual Stress and Input Description of the Code, Pacific Northwest Laboratory, Richland, Washington.

VISA, 1983, ”VISA - A Computer Code for Predicting the Probability of Reactor Pressure Vessel Failure,” Pacific Northwest Laboratory, Richland, Washington.

Wallin, K., 1999, “Application of the Master Curve Method to Crack Initiation and Crack Arrest,” PVP-Vol. 393, ASME, New York, New York.

Table 2. A Comparison of the Current PTS and the Master Curve Methodologies - Hypothesis 1

Parameter	Current			Master Curve		
Reference Temp.	Initial RT_{NDT}			T_0 (RT_{T0})		
		Generic Data	Plant-specific Data		Generic Data	Plant-specific Data
	Mean	56°F	Measured Initial RT_{NDT}	Mean	Kirk's work	Measured T_0
	σ_I	17°F	0°F	σ_I	27°F (EPRI TR-108390, Rev. 1)	$\geq\sigma_{T0}$ by ASTM E-1921-97
Shift	$\triangle RT_{NDT}$			$\triangle T_0$ ($\triangle RT_{T0}$)		
		Generic Data	Plant-specific Data		Generic Data	Plant-specific Data
	Mean	Trend Curve of RG. 1.99, Rev. 2	Measured $\triangle RT_{NDT}$	Mean	Trend Curve of RG. 1.99, Rev. 2 (Basis of this hypothesis)	Measured $\triangle T_0$
	$\sigma_\triangle$	28°F	14°F	$\sigma_\triangle$	Kirk's work	------
Screening Criteria	270°F			---		
Limiting Vessel Failure Frequency	$5x10^{-6}$			---		

Proceedings of ICONE 8
8th International Conference on Nuclear Engineering
April 2-6, 2000, Baltimore, MD USA

ICONE-8010

THE APPLICABILITY OF THIN-WALL LIMIT-LOAD SOLUTIONS TO STAINLESS STEEL PIPING USED IN THE NUCLEAR INDUSTRY

Simon C. F. Sheng
U.S. Nuclear Regulatory Commission
Material and Chemical Engineering Branch
7D4, OWFN, USNRC, Washington D.C. 20555
Phone: (301) 415-2708
Fax: (301) 415-2444
E-mail: SHENG@NRC.GOV

ABSTRACT

Although the thick-wall limit-load solutions for pipes with inner flaws have been available for some time, thin-wall solutions have been used for almost all applications throughout the nuclear industry. So far, very little work has been done to explore the applicability of thin-wall limit load solutions to a variety of stainless steel piping under various loading conditions. This paper will use a typical 12-inch surge line made of Type 316 stainless steel as an example to study the applicability of the thin-wall limit-load solutions to a potentially thick-wall piping. The objective is to find out whether or not the thin-wall limit-load solutions can generate satisfactory results for this typical surge line so that the errors associated with using the thin-wall solutions can be assessed for stainless steel pipes of other schedules with various radius to thickness ratios. The study covers the thick-wall limit-load solutions available in the literature for pipes with inner flaws and those derived by the author for pipes with outer flaws. The effect of loading types, such as tension or bending load only, or the combined load of tension and bending, to the applicability of thin-wall limit-load solutions will also be explored in this paper.

INTRODUCTION

The subject of limit load analysis for piping containing a circumferential through-wall crack or a circumferential part-through crack located at the inside of the pipe wall (inner crack) has been studied extensively for tension, bending, and the combined load of tension and bending as summarized in Miller's paper (1988). The most general equation presented there was the limit load solution derived by Kanninen et al. (1982) for a thick-wall pipe with an inner crack under the combined load of tension and bending. Sheng (1999) expanded Miller's work and published his limit load solution for a circumferential part-through crack located at the outside of the pipe wall (outer crack) for the combined load of tension and bending. Both Kanninen's solution for the inner crack and Sheng's solution for the outer crack were for a thick-wall piping with a crack not penetrating the compressive side of the pipe under combined loads.

Since Kanninen's solution for combined loads cannot be reduced to that of Zahoor (1984) for the special case of a part-through inner crack on a thick-wall pipe under tension, Sheng revisited Kanninen's solution and derived his version of the limit load solution for a thick-wall pipe with an inner carck. It should be noted that Sheng's limit load solution for inner cracks under combined loads can be reduced to Zahoor's solution for tension. Further, Sheng has carried out simplifications and presented limit load solutions for cases of: (1) tension only, (2) bending only (3) part-through flawed thin-wall pipes, (4) through-wall flawed thin-wall pipes, and (5) a composite crack geometry, i.e., a 360-degree inner part-through crack.

This paper continue Sheng's work of 1999 to study the applicability of the thin-wall limit-load solutions to a variety of stainless steel piping commonly used in the nuclear industry. The objective is to provide a somewhat bounding error estimate for using the thin-wall limit-load solutions to potentially thick-wall pipes. The study covers the thick-wall limit-load solutions for pipes with an inner flaw and pipes with an outer flaw. The effect of loading types, such as tension or bending only, or

combined tension and bending, to the applicability of thin-wall limit-load solutions will also be explored in this paper.

Since this paper only deals with finite flaws in the circumferential direction, the author dropped the term "circumferential" for simplicity in describing crack geometry later on. Also, since inner or outer cracks explicitly mean part-through cracks, the term "part-through" will also be dropped when we mention inner or outer cracks.

ANALYTICAL MODELS

Figure 1 shows the schematic of a pipe cross section containing an inner crack, and Fig. 2 shows the schematic of a pipe cross section containing an outer crack. The crack depth, a, and the half angle of the crack length, θ, are parameters related to the crack geometry. The pipe thickness, t, and the outer radius R_o are parameters related to the pipe geometry. The figures also show the angle, γ, which is a parameter determining the location of the neutral axis of the pipe cross section.

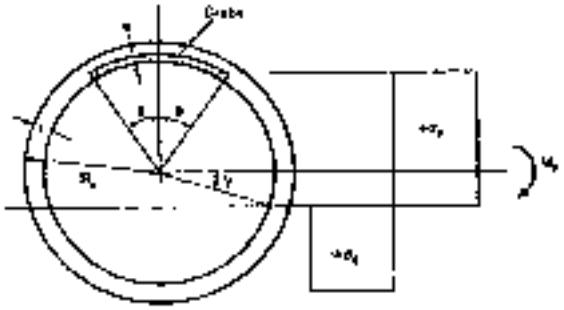

Figure 3 The Schematic of an Inner Crack on a Thick-wall Pipe

For the thick-wall piping, the limit load solution derived by Sheng is

$$\frac{M_b}{2\sigma_o R_o^2 t} = (1+\lambda)\left(1-\zeta+\frac{\zeta^2}{3}\right)\cos\gamma - x\left(1-2\zeta+\zeta^2+x\zeta-x\zeta^2+\frac{\lambda}{\quad}\right) \quad \textbf{(1)}$$

and

$$\frac{P}{\sigma_o(1+\lambda)\left(1-\frac{\zeta}{2}\right)\pi R_o t} = \frac{1-\lambda}{1+\lambda}+\frac{2\gamma}{\pi}-\frac{2}{1+\lambda}\left(\frac{x\theta}{\pi}\right)\frac{2-2\zeta+x\zeta}{2-\zeta} \quad \textbf{(2)}$$

for a pipe with an inner crack as depicted in Fig. 1. Equation (1) is derived from the moment balance across the section, and Eq. (2) is from the force balance. These equations are for thick-wall flawed pipes because in the integration of the moment, M_b, and force, P, over the pipe cross section, the radius r and the angle θ were treated as independent variables and were placed inside the integration sign. Also, no simplification such as $t/R_o << 1$ was used.

Parameters x and ζ in Eqs. (1) and (2) are defined as x = a/t and ζ = t/ R_o. Parameters, σ_o and λ, are material parameters. Parameter σ_o is flow stress, which is usually taken as the average of the yield and ultimate stresses or three times the ASME Code design stress intensity, S_m. Parameter λ is the ratio of the flow stress in compression to the flow stress in tension. It should be noted that the cross sectional area of the pipe may take different forms, for instance, $2(1-\zeta/2)\pi R_o t$ is identical to $\pi(R_o^2 - R_i^2)$, where R_i is the inner radius of the pipe.

Equation (1) is different from Kanninen's moment balance equation, however, Eq. (2) can be transformed to the identical form of Kanninen's force balance equation. This difference will be discussed later in Discussion. The corresponding limit load solution derived by Sheng for a pipe with an outer crack depicted in Fig. 2 is

$$\frac{M_b}{2\sigma_o R_o^2 t} = (1+\lambda)\left(1-\zeta+\frac{\zeta^2}{3}\right)\cos\gamma - x\left(1-x\zeta+\frac{x^2\zeta^2}{3}\right)\sin\theta \quad \textbf{(3)}$$

and

$$\frac{P}{\sigma_o(1+\lambda)\left(1-\frac{\zeta}{2}\right)\pi R_o t} = \frac{1-\lambda}{1+\lambda}+\frac{2\gamma}{\pi}-\frac{2}{1+\lambda}\left(\frac{x\theta}{\pi}\right)\frac{2-x\zeta}{2-\zeta} \quad \textbf{(4)}$$

LIMIT LOAD SOLUTIONS FOR SPECIAL CASES

With the limit load solutions available for thick-wall pipes, limit load solutions for special cases can be derived easily. Since the objective of this paper is to examine the applicability

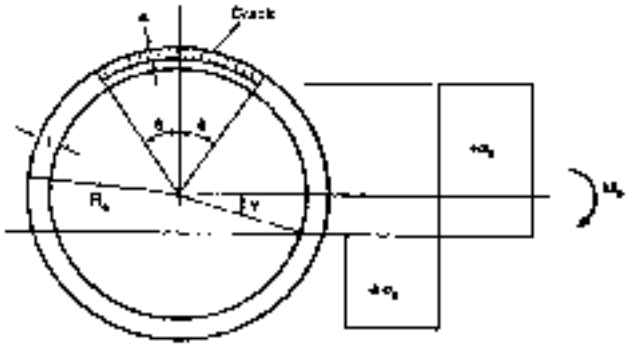

Figure 4 The Schematic of an Outer Crack on a Thick-wall Pipe

of using thin-wall limit load solutions to thick-wall pipes, the author only reference the limit load solutions for the first three special cases of Sheng's work. For completeness, they are reproduced below.

Case 1: Part-Through Flawed Thick-Wall Pipe Under Tension

For an inner flaw, after setting $M_b = 0$ for pure tension, Eq. (1) becomes:

$$\cos\gamma = \frac{1}{1+\lambda}\,\frac{x\left(1-2\zeta+\zeta^2+x\zeta-x\zeta^2+\frac{x^2\zeta^2}{3}\right)}{\left(1-\zeta+\frac{\zeta^2}{3}\right)}\sin\theta \qquad \textbf{(5)}$$

In this application, Eq. (2) remains the same.

For an outer flaw, Eq. (3) becomes:

$$\cos\gamma = \frac{1}{1+\lambda}\,\frac{x\left(1-x\zeta+\frac{x^2\zeta^2}{3}\right)}{\left(1-\zeta+\frac{\zeta^2}{3}\right)}\sin\theta \qquad \textbf{(6)}$$

And Eq. (4) remains the same. It should be noted that the above two equations can be simplified further by setting $\lambda = 1$ when the flow stresses for tension and compression are equal.

Case 2: Part-Through Flawed Thick-Wall Pipe Under Pure Bending

For an inner flaw, after setting P = 0 for pure bending, Eq. (1), the moment balance equation, remains unchanged. However, Eq. (2) becomes:

$$\gamma = -\frac{\pi}{2}\frac{1-\lambda}{1+\lambda} + \frac{x\theta}{1+\lambda}\frac{2-2\zeta+x\zeta}{2-\zeta} \qquad \textbf{(7)}$$

For an outer flaw, Eq. (3) remains unchanged, and Eq. (4) becomes,

$$\gamma = -\frac{\pi}{2}\frac{1-\lambda}{1+\lambda} + \frac{x\theta}{1+\lambda}\frac{2-x\zeta}{2-\zeta} \qquad \textbf{(8)}$$

Case 3: Part-Through Flawed Thin-Wall Pipe Under Combined Loading

For thin-wall pipes, $t/R_o << 1$, therefore, the corresponding limit load solutions can be obtained by setting $\zeta = 0$ in Eqs. (1) to (4). As expected, both the inner-crack and outer-crack equations reduced to the same simplified form:

$$\frac{M_b}{2\sigma_o R^2 t} = (1+\lambda)\cos\gamma - x\sin\theta \qquad \textbf{(9)}$$

and

$$\frac{P}{\sigma_o(1+\lambda)\pi Rt} = \frac{1-\lambda}{1+\lambda} + \frac{2\gamma}{\pi} - \frac{2}{1+\lambda}\left(\frac{x\theta}{\pi}\right) \qquad \textbf{(10)}$$

The author used R, which is defined as: $R = 0.5\,(R_i + R_o)$, instead of R_o for the radius of the thin-wall pipe in Eqs. (9) and (10) because it is no longer meaningful to differentiate R from R_i or R_o for thin-wall pipes.

NUMERICAL RESULTS

Simulations have been performed using Eqs. (1) to (10) to study the applicability of thin-wall limit load solutions to thick-wall pipes. All simulations assume that the flow stresses for tension and compression are equal, i.e., $\lambda = 1$. The numerical results are plotted in Figs. 3 to 9 for a typical 12-inch surge line of Schedule 160 (t = 1.312 inches and outer diameter = 12.75 inches) for a typical pressurized water reactor. Figure 3 plots the results for Case 1 using Eqs. (2) and (5) for a pipe with an inner flaw, and Fig. 4 plots the results using Eqs. (4) and (6) for a pipe with an outer flaw. Both figures show the variation of the normalized P (tension) from the thick-wall solution and the thin-wall solution as a function of θ for x of 0.25, 0.50, and 1.0. The normalized P is defined as $P/(2\pi\sigma_o Rt)$. It should be noted that for all numerical simulations using Eqs. (1) to (8) for thick pipes, normalization of P was made with respect to R, not R_o, so that direct comparison could be made with results using thin-wall solutions. Results for Case 2 using Eqs. (1) and (7) for a pipe with an inner flaw, and using Eqs. (3) and (8) for a pipe with an outer flaw are shown in Figs. 5 to 9. Since Case 2 represents a special case (normalized P = 0) for the combined load of tension and bending to be discussed later, no more discussion will be given here.

Simulations have been performed for combined tension and bending represented by Eqs. (1) to (4) for the thick-wall pipes and Eqs. (9) and (10) of Case 3 for thin-wall pipes. For Figs. 5 to 9, instead of the normalized P, the plots show the normalized M (moment) from both the thick-wall solution and the thin-wall solution as a function of θ for various normalized P values. The normalized M is defined as $M/(4\sigma_o R^2 t)$ in terms of R for the same reason given above. Specifically, Fig. 5 shows the variation of $M/(4\sigma_o R^2 t)$ as a function of θ for $P/(2\pi\sigma_o R t)$ values of 0, 0.25, and 0.50 for x = 0.25, for the inner flaw case. For each $P/(2\pi\sigma_o R t)$ value, there are two curves in Fig. 5: (1) a plot of results for using the thick-wall solution and (2) a plot of results for using the thin-wall solution. It should be noted that the dashed line curve is based on Eqs. (1) and (2) and the solid line curve is based on Eqs. (9) and (10). Similarly, Fig. 6 shows the variation of $M/(4\sigma_o R^2 t)$ as a function of θ for $P/(2\pi\sigma_o R t)$ values of 0, 0.25, and 0.50 for x = 0.25, for the outer flaw case. Here, the dashed line curve is based on Eqs. (3) and (4) and the solid line curve is again based on Eqs. (9) and (10).

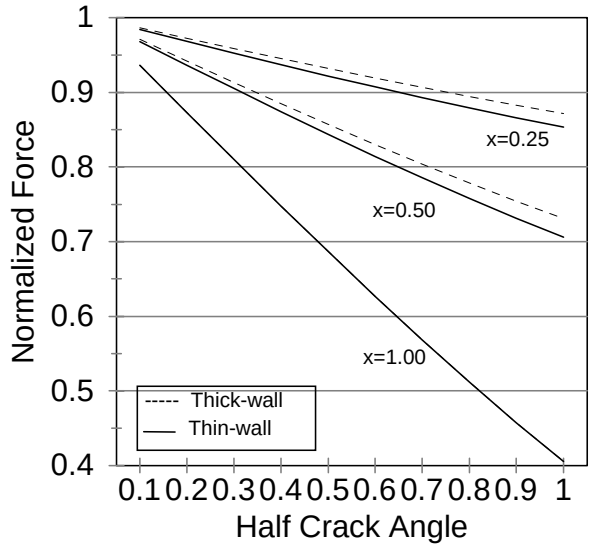

Figure 5 The Limit Force for a Pipe with an Inner Flaw - Tension Only

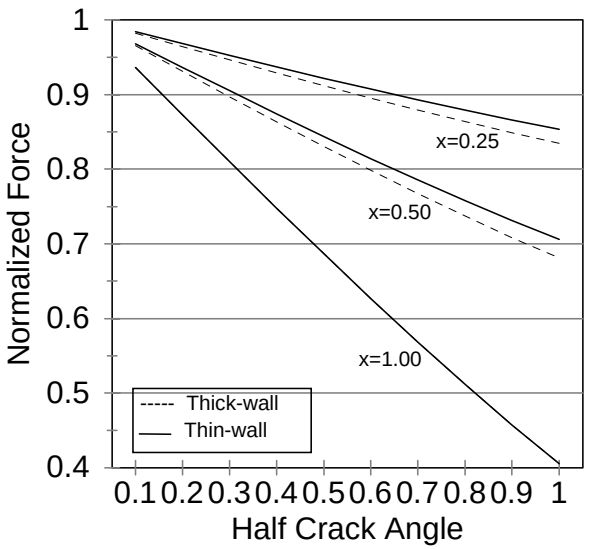

Figure 4 The Limit Force for a Pipe with an Outer Flaw - Tension Only

Similar results are presented in Figs. 7 and 8 for x equal to 0.5 and Fig. 9 for x equal to 1.0.

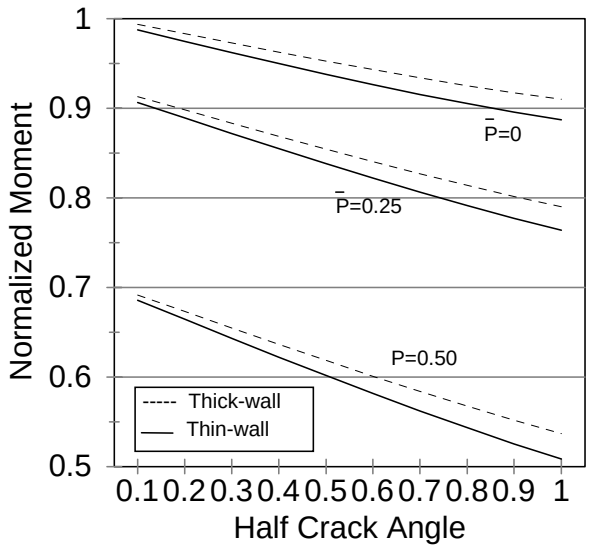

x = 0.25

Figure 5 The Limit Moment for a Pipe with an Inner Flaw - Tension and Bending for x=0.25

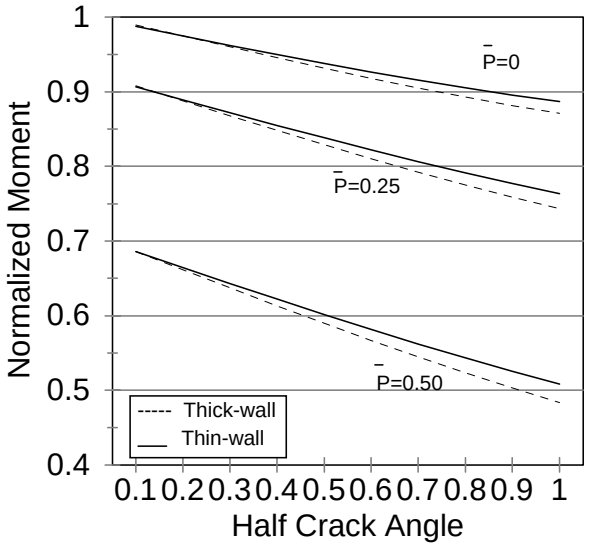

x = 0.25

Figure 6 The Limit Moment for a Pipe with an Outer Flaw - Tension and Bending for x=0.25

Setting $\lambda = 1$ and noting that x in Equations (9) and (10) is simply a/t, we can transform Equations (9) and (10) into

$$P'_b = \frac{6S_m}{\pi}\left(2\sin\beta - \frac{a}{t}\sin\theta\right) \qquad \textbf{(11)}$$

and

DISCUSSION

The notations for all equations presented here are consistent with those in the majority of the publications on the subject of limit load analysis. However, they are not the same as those in Appendix C of Section XI of the ASME Code. To make a comparison of Equations (9) and (10) to those in the ASME Code, the author defines $P'_b = M_b/(\pi R^2 t)$, $P_m = P/(2\pi Rt)$, $\sigma_o = 3S_m$ (for austenitic piping), and $\beta = \pi/2 - \gamma$ to establish the relationship between the two different sets of notations.

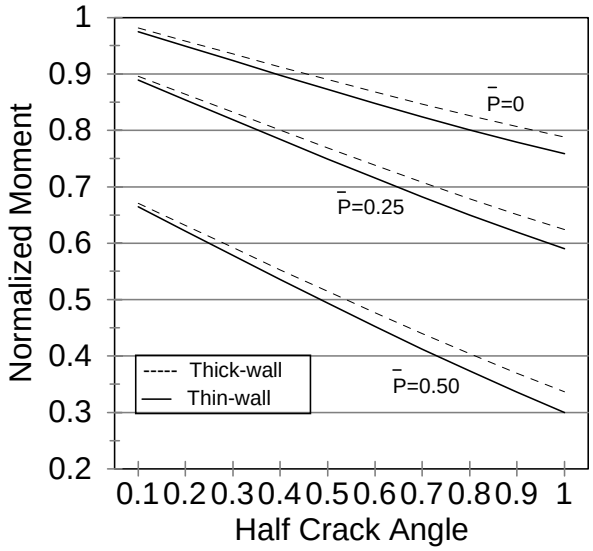

x = 0.50

Figure 7 The Limit Moment for a Pipe with an Inner Flaw - Tension and Bending for x=0.50

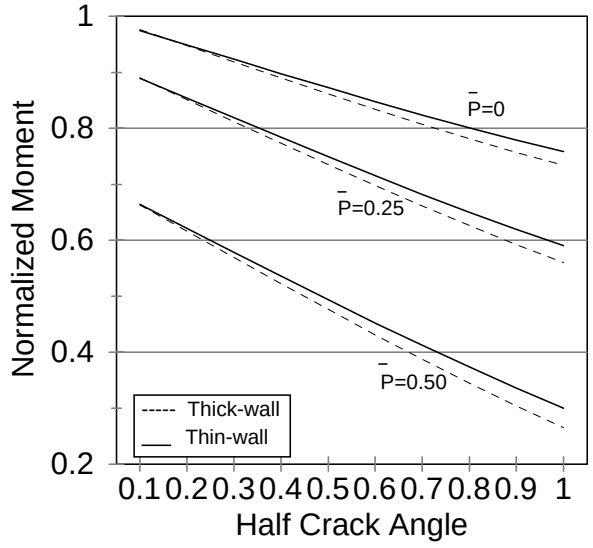

x = 0.50

Figure 8 The Limit Moment for a Pipe with an Outer Flaw - Tension and Bending for x=0.50

$$\beta = \frac{1}{2}\left(\pi - \frac{a}{t}\theta - \pi\frac{P_m}{3S_m}\right) \qquad \textbf{(12)}$$

These are exactly the same as those in Appendix C of the ASME Code. In addition, the equations presented n this paper can be reduced to Zahoor's solution for tension only (Equation 5).

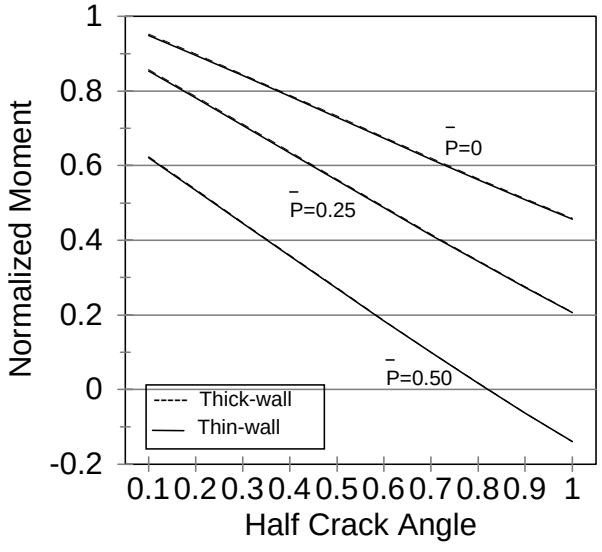

x = 1.00

Figure 9 The Limit Moment for a Pipe with a Through Wall Flaw - Tension and Bending for x=1.0

The numerical results indicated that using thin-wall solutions is conservative for pipes with an inner flaw and non-conservative for pipes with an outer flaw. The error in the predicted limit force for either the inner flaw or outer flaw case under pure tension increases with the flaw depth until x reaches approximately 0.5. The error starts to decrease from this point until x reaches 1.0. The largest error is 3.5% for either the inner flaw or outer flaw case for a half through flaw (x=0.5). For the combined load of tension and bending, the error in the predicted limit moment for either the inner flaw or outer flaw case increases with the flaw depth until x reaches approximately 0.5 and increases with the normalized force. The error also starts to decrease from this point (x=0.5 approximately) until x reaches 1.0. The largest error is 12.6% for the inner flaw case and 12% for the outer flaw case under a normalized force of 0.5 for a half through flaw. As expected, the error is negligible for a pipe with a through-wall flaw (x = 1.0) for all cases studied here.

CONCLUSIONS

Based on the limit load solutions developed by the author in 1999 for thick-wall piping with either an inner flaw or an outer flaw, the author performed a numerical evaluation to study the applicability of thin-wall limit load solutions to a typical 12-inch, Schedule 160, surge line made of Type 316 stainless steel. This work indicated that using thin-wall solutions is conservative for pipes with an inner flaw and non-conservative for pipes with an outer flaw. The largest error is 3.5% for either the inner flaw or outer flaw case under pure tension. The largest error is 12.6% for the inner flaw case and 12% for the outer flaw case under a normalized force of 0.5 for a half through flaw. Since the piping chosen for the study is quite thick ($t/R_o = 0.2058$), These error estimates might be

considered as bounding values for most of the stainless piping used in the nuclear industry.

REFERENCES

Kanninen, M.F., Zahoor, A., Wilkowski, G., Abou-Sayed, I., Marshall, C., Broek, D., Sampath, S. Rhee, H., and Ahmad, J., 1982, "Instability Predictions for Circumferentially Cracked Type 304 Stainless Steel Pipes Under Dynamic Loading," EPRI NP-2347, Vols 1 and 2, EPRI, USA.

Miller, A.G., 1988, "Review of Limit Loads of Structures Containing Defects," Int. J. Pres. & Piping, 32 (197-327).

Sheng, C.F., 1999, "The Limit-Load Solution for a Thick-wall Pipe with a Circumferential Crack Under Combined Tension and Bending Loads," PVP-Vol. 388, ASME, New York, New York.

Zahoor, A. and Norris, D.M., 1984, "Ductile Fracture of Circumferentially Cracked Type-304 Stainless Steel Pipes in Tension," ASME Journal of Pressure Vessel Technology, November 1984, Vol. 106 (399-400).